

Influence of Implant Surface Topography and Loading Condition on Stress Distribution in Bone Around Implants: A Comparative 3D FEA

Ravindra C. Savadi · Jatin Agarwal ·
Rolly Shrivastava Agarwal · V. Rangarajan

Received: 1 June 2011 / Accepted: 3 October 2011 / Published online: 19 October 2011
© Indian Prosthodontic Society 2011

Abstract A three-dimensional Finite Element Method was used to study the influence of porous coated surface topography of an implant on stress and strain distribution pattern in the cortical and cancellous bone during axial and non-axial loading. Two implants, one with porous surface topography and one with smooth surface were embedded in separate geometric models of posterior mandibular region which was generated using a CT scan data. Material properties and boundary conditions were applied. Load of 100 and 50 N were applied on to the abutment from axial and non-axial directions respectively. Porous surface topography appeared to distribute stress in a more uniform pattern around the implant with near absence of stress in the apical region of implant. Smooth surfaced implant showed high punching stress at the apex of the implant. The porous coated interface was considered to simulate the

shock absorbing behavior of periodontal ligament of natural dentition. Maximum amount of stress concentration was observed in the cortical bone which plays a major role in the dissipation of the stress.

Keywords Cortical bone · Implant · Porous surface topography · Smooth surface topography · 3D FEA

Introduction

A new era in oral rehabilitation began with the introduction of osseointegrated dental implants [1]. The high success rates and long term follow up of patients treated with osseointegrated dental implants for more than 20 years have interested clinicians and researchers worldwide [2]. Despite the high success rates reported to date, implant failures do occur. The reasons for failure of implants are poor oral hygiene, poor bone quality, compromised medical status of the patient and biomechanical factors.

Various authors have stressed the importance of biomechanical factors such as type of loading, the bone–implant interface, the length and diameter of the implants, the shape and characteristics of the implant surface, the prosthesis type and the quantity and quality of the surrounding bone [3]. Inappropriate loading causes excessive stress in the bone around the implant and may result in bone resorption. The long-term function of a dental implant system will depend on the biomechanical interaction between bone and implant which controls the state of stress in surrounding tissues.

Studies have shown that the close apposition of bone to the titanium implant is an essential feature that allows transmission of stress from the implant to the bone without any appreciable relative motion or abrasion [4]. In case of a smooth surface implant, a strong bond between implant

R. C. Savadi
Department of Prosthodontics, Oxford Dental College,
Bangalore, India
e-mail: rcsavadi@gmail.com

J. Agarwal (✉)
Department of Prosthodontics, College of Dental Science &
Hospital, Rau, Indore, India
e-mail: dentalperfectionclinic@gmail.com

J. Agarwal
A/9, Basant Vihar, Bh. Satya Sai school, A.B. road, Indore,
Madhya Pradesh 452010, India

R. S. Agarwal
Department of Conservative Dentistry, College of Dental
Science & Hospital, Rau, Indore, India

V. Rangarajan
Department of Prosthodontics, Sri Venkateshwara Dental
College, Chennai, India

surface and bone is not present for satisfactory performance. However, an implant surface with roughness [5] and porosity may have a beneficial interlocking effect to achieve osseointegration, resulting in favorable stress distribution [4].

Thus in this study surface topography of a root form implant is chosen as a parameter to understand the effect of loads on the bone through the implant.

The finite element technique offers the potential of evaluating and improving implant design without the risk and expense of implantation.

Therefore, a three-dimensional finite element analysis method was used to understand the behavior of bone around the porous rooted dental implant as well as the mechanism of stress transfer through the interface when it is loaded under axial and non-axial directions.

Materials and Methods

In this study, a section of mandible of lower first molar region of a length 25.6 mm (mesio-distally) [6, 7] was taken from the CT scan and converted into a three dimensional solid model for analysis purpose using ANSYS Pre-processor (ANSYS version 8.0 software) (Fig. 1 3D solid model of the bone segment). A three-dimensional model of Endopore Implant (Innova corporation, Toronto) [8–11] with dimensions of 4.1 mm diameter and 12 mm length with a 1 mm smooth coronal region with a suitable abutment was generated [12] (Fig. 2 3D solid model of implant with abutment). The geometry of the implant design with its surface topography was provided by the manufacturer (Innova corporation, Toronto). The implant considered was of truncated root form with a 5° taper [8, 11]. Coronally the 1 mm smooth surface of the implant

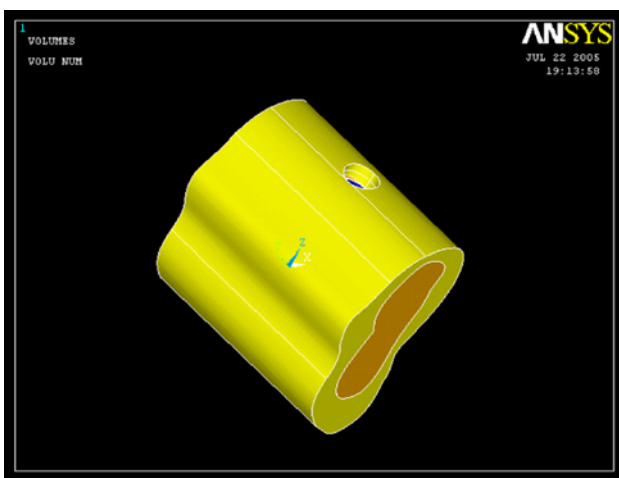


Fig. 1 3D solid model of the bone segment

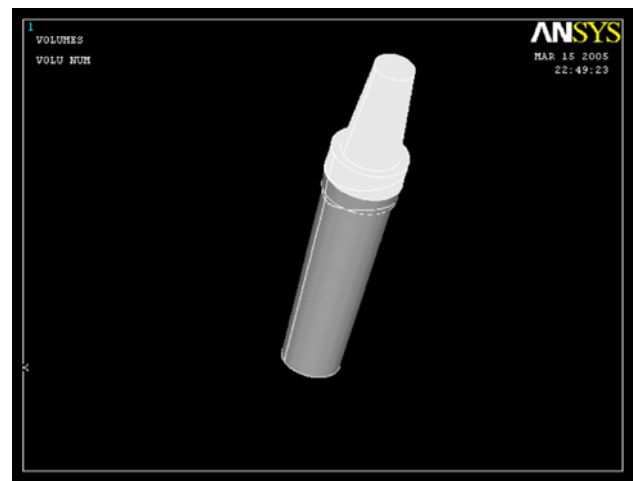


Fig. 2 3D solid model of implant with abutment

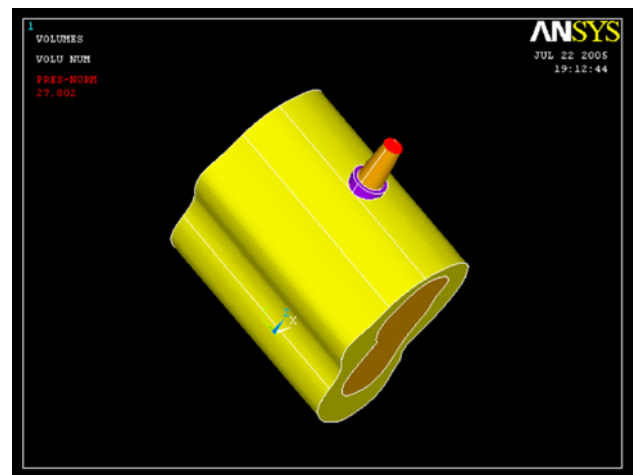


Fig. 3 Insertion of implant with respect to the section of bone

coincided with the cortical bone (Fig. 3 Insertion of implant with respect to the section of bone). Except for the 1 mm smooth coronal region, the rest of the surface of the implant was occupied by diffusion bonded microsphere surface (Fig. 4 Model of implant with microspheres) [10]. The implant was assumed to be placed in the region of first molar of the mandible [13].

Another implant of the same dimensions but with the smooth surface i.e. without interface properties was also modeled and placed in similar section of mandible for comparison. The height and diameter of abutment was also kept the same. The models were provided in close approximation to the *in vivo* geometry.

The section of bone containing implant with smooth surface was considered as Model 1 and the one with porous surface topography as Model 2.

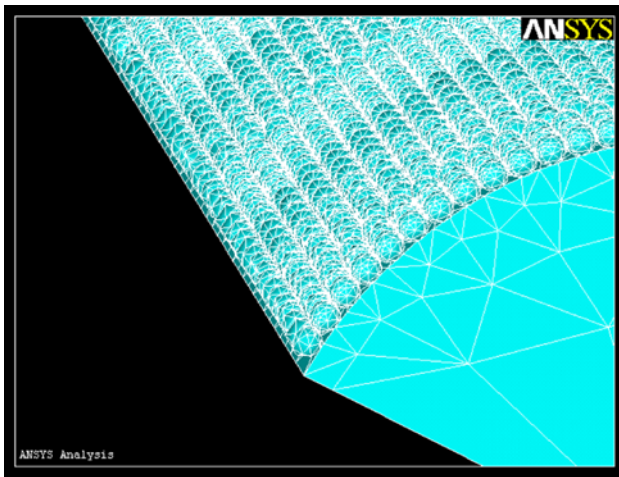


Fig. 4 Model of implant with microspheres

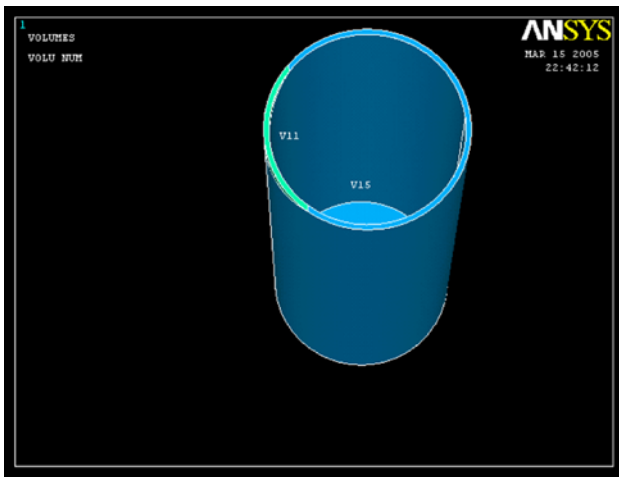


Fig. 5 Model of implant bone ingrowth bonded interface

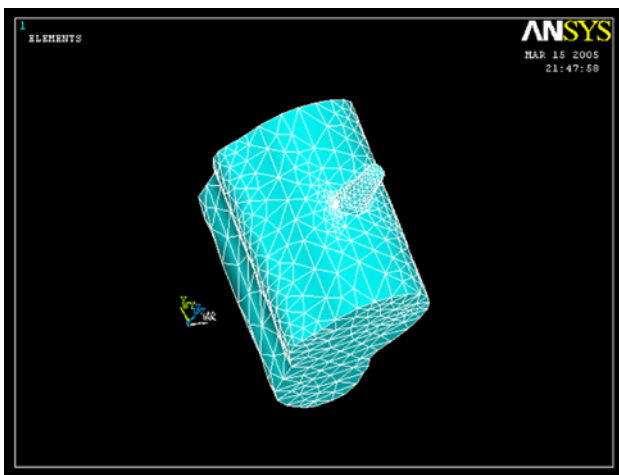


Fig. 6 3D finite element model with meshing

Modeling of the Interface

The implant was designed as a solid machined core surrounded by porous coating consisting of two to three layers of microspheres. These microspheres have an average diameter of $100\ \mu\text{m}$, thus giving a porous coating of $300\ \mu\text{m}$ thickness [9]. The diameter of microsphere was chosen so that the resulting pore size created a space between two microspheres, which would be amenable to bone ingrowth [14]. Since this geometry was impossible to implement due to smaller grid size used, an analogous set of interface properties was developed. A row of thin interface elements was placed between the porous surface of implant and the bone to provide a means of modeling the interface region associated with bone in growth (Fig. 5 Model of implant bone ingrowth bonded interface). According to the studies done by Cook et al. [15], it was assumed that the bone could be approximated by small cantilever beams in the porous section of the implant at the interface. To relate this to the Finite Element Model, the interface element was assumed to be a rectangular cantilever beam of uniform dimension between the implant and the bone.

Mesh Generation

The three-dimensional finite element model corresponding to the geometric model was meshed using ANSYS Pre-processor (ANSYS version 8.0 software). The type of meshing is free meshing because the model is not geometrically symmetric (Fig. 6 3D finite element model with meshing). The element size (SOLID 187) was selected according to default settings (Fig. 7 Solid 187 type element). The type of element suitable for this particular study was 10 noded tetrahedron element which was assigned three degrees of freedom per node, namely translation in the x, y and z directions. The elements were constructed so that their size aspect ratio would yield reasonable solution accuracy.

Specifying Material Properties

For the execution and accurate analysis of the program two material properties were utilized i.e. Young's modulus and Poisson's ratio.

The cortical bone, cancellous bone and implant with abutment were presumed to be linearly elastic, homogeneous and isotropic [6, 16]. Although cortical bone has anisotropic [17] material characteristics and possesses regional stiffness variation, they were modelled isotropically. The mechanical properties of the interface material (bone ingrown into porous implant surface) were mathematically calculated, assuming it to be a composite material [18].

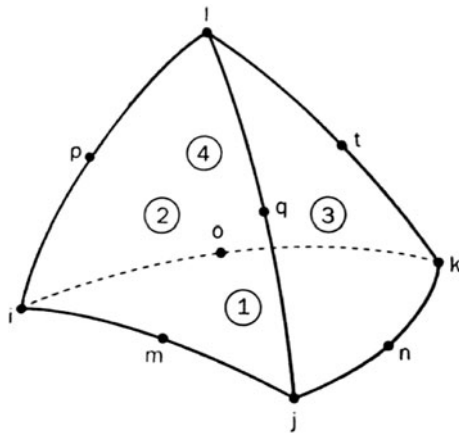


Fig. 7 Solid 187 type element

Table 1 Mechanical properties of different materials used in the Model

Material	Young’s modulus (Mpa)	Poisson’s ratio
Cortical bone [14, 17]	13700	0.30
Cancellous bone [6, 16, 17]	1370	0.30
Implant (Titanium alloy) [20]	110000	0.35
Interface [15]	55750	0.35

According to the mathematical equation, interface material is a composite of Young’s modulus of different materials such as the titanium alloy and bone. The Young’s modulus of the whole system as composite is calculated considering an Iso-Strain condition. This condition assumes a uniform strain on both the implant and bone portions of the composite. Thus bonding between the implant and bone remains intact during the application of stress.

The Young’s modulus of the composite is derived in terms of the elastic modulus and the volume fraction of the implant and bone.

The load on the composite is equal to the sum of the load on the implant and the load on the bone.

$$\text{Therefore, } P_C = P_I + P_B,$$

where, P_C is the load on the composite, P_I is the load on the implant, P_B is the load on bone.

$$\text{We have, } \sigma = \frac{P}{A} \text{ or } P = \sigma A$$

where, σ is the stress, P is the load, A is the area

$$\text{The final equation is, } E_c = E_b V_b + E_i V_i$$

where, E_c is the Young’s Modulus of composite, E_b is the Young’s Modulus of bone, E_i is the Young’s Modulus of implant

The corresponding elastic properties such as Young’s Modulus (E) and Poisson’s ratio (ν) of cortical bone,

cancellous bone and implant were determined according to literature survey [17, 19]. (As shown in Table 1).

Applying Boundary Conditions

Constraints were applied on the distal end of the model in all the three axes [20–22] (Fig. 8a Application of constraints (distal surface of the model)) omitting support at the bottom permitted bending of the model [7, 23]. These aspects make the model a more realistic representation of the clinical situation [24].

Application of Loads

The magnitude of applied loads was within physiologic limits (Fig. 8b Application of load on top surface of the

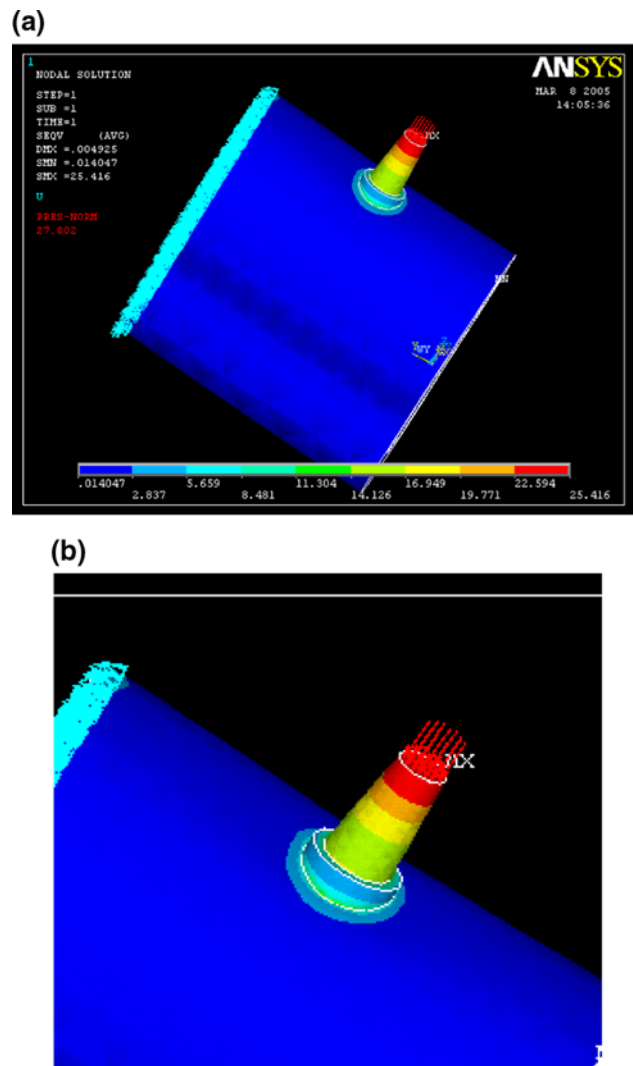


Fig. 8 a Application of constraints (distal surface of the model). **b** Application of load on top surface of the abutment (parallel dotted lines)

Table 2 Grouping of models based on the direction and magnitude of forces and surface topography of the implants

Groups	Forces	Direction	Model (smooth surface)	Model (rough surface)
Group 1	100 N	Axial	Model 1	Model 2
Group 2	50 N	Bucco-Lingual	Model 1	Model 2
Group 3	50 N	Mesio-Distal	Model 1	Model 2

abutment (parallel dotted lines)) [25, 26] and direction of application of the loads simulated the clinical conditions [27].

An axial load of 100 N was directly applied onto the abutment [3, 28–30]. The prosthesis was not modeled for ease of fabrication of model and also for simplification of interpretation of results.

A non-axial load of 50 N was applied onto the abutment from buccolingual direction.

A non-axial load of 50 N was applied onto the abutment from mesiodistal direction.

A total of two models were made and grouped into three for the ease of analysis. (Table 2).

Finite Element Analysis

These different models were analyzed by Processor i.e. solver and the results were displayed by Post-Processor of the Finite Element Software (ANSYS, version 8.0) in the form of color-coded maps using Von Mises Stress Analysis.

Results

Stress was calculated using Von Mises criteria, which represented the distribution of stress in color coded maps. Dark blue color represents area with minimal stress while red color represents area with maximum stress. Tables 3, 4, 5, 6, 7 represents Von Mises stress (in MPa) and Von Mises strain (in microns) generated in different components of the models.

Table 3 Von Mises stress (in MPa) in the cortical bone under different masticatory forces

Groups	Model 1	Model 2
Group 1 (Axial forces 100 N)	11.739	13.674
Group 2 (Bucco-lingual forces 50 N)	32.077	37.122
Group 3 (Mesio-distal forces 50 N)	18.406	35.648

Table 4 Von Mises stress (in MPa) in the cancellous bone under different masticatory forces

Groups	Model 1	Model 2
Group 1 (Axial forces 100 N)	1.473	1.387
Group 2 (Bucco-lingual forces 50 N)	1.016	1.631
Group 3 (Mesio-distal forces 50 N)	1.203	1.303

Table 5 Von Mises strain (in microns) in the cancellous bone under different masticatory forces

Groups	Model 1	Model 2
Group 1 (Axial forces 100 N)	9.83×10^{-4}	9.28×10^{-4}
Group 2 (Bucco-lingual forces 50 N)	6.8×10^{-4}	10.8×10^{-4}
Group 3 (Mesio-distal forces 50 N)	8.06×10^{-4}	8.69×10^{-4}

Table 6 Von Mises stress (in MPa) on interface (bone–implant) with different masticatory forces

Groups	Model 2
Group 1 (Axial forces 100 N)	6.669
Group 2 (Bucco-lingual forces 50 N)	21.535
Group 3 (Mesio-distal forces 50 N)	21.631

Table 7 Von Mises stress (in MPa) in the implant with abutment under different masticatory forces

Groups	Model 1	Model 2
Group 1 (Axial forces 100 N)	25.53	25.41
Group 2 (Bucco-lingual forces 50 N)	121.406	115.164
Group 3 (Mesio-distal forces 50 N)	107.217	106.282

Cortical Bone

Irrespective of the model and loading condition, maximum amount of Von Mises stress was found in the cortical bone concentrated at the area adjacent to the implant abutment junction. On axial loading, stress values were comparable between Model 1 and Model 2 (Table 3), while more uniform stress distribution pattern was generated in Model 2 (Fig. 9b Von Mises stress in cortical bone of Model 2, Group 1) as compared to Model 1 (Fig. 9a Von Mises stress in cortical bone of Model 1, Group 1). During non axial loading, the stresses generated in the Model 2 were slightly higher as compared to Model 1 (Table 3).

Cancellous Bone (Stress and Strain)

On axial loading, a slight decrease in stress value was observed in Model 2 as compared to Model 1 (Table 4).

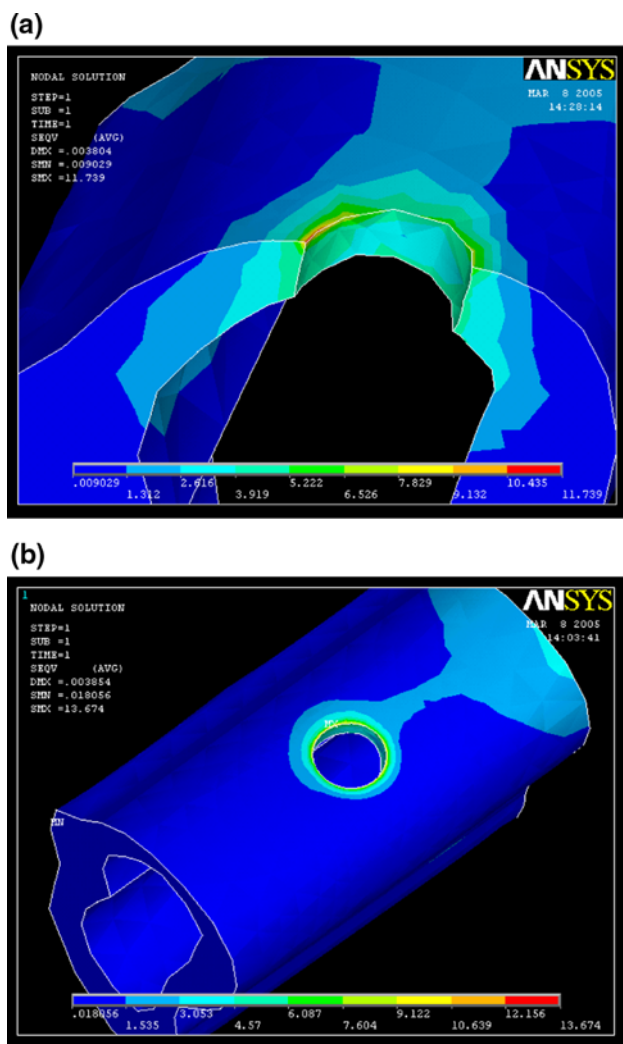


Fig. 9 a Von Mises stress in cortical bone of Model 1, Group 1. b Von Mises stress in cortical bone of Model 2, Group 1

Figure 10a shows Von Mises stress in cancellous bone of Model 1, Group 1 that maximum stress was concentrated at the base of the implant while Fig. 10b shows Von Mises stress in cancellous bone of Model 2, Group 1 that the stress was localized to the coronal half region of implant and minimal stress was found at the apical half. Von Mises strain values for Model 2 (Table 4) were comparatively lesser with deformation present only in the coronal half of bone segment (Fig. 11b Von Mises strain in cancellous bone of Model 2, Group 1), unlike that in Model 1 where deformation occurred at the apical half of implant (Fig. 11a Von Mises strain in cancellous bone of Model 1, Group 1). During non axial loading Von Mises stress and strain values were higher for Model 2 as compared to Model 1 (Tables 4 and 5). The stress was mainly distributed in the coronal region of implant, depending on the direction of loading (Figs. 12a and b showing Von Mises stress in cancellous bone of Model 1, Group 2 and Group 3, respectively).

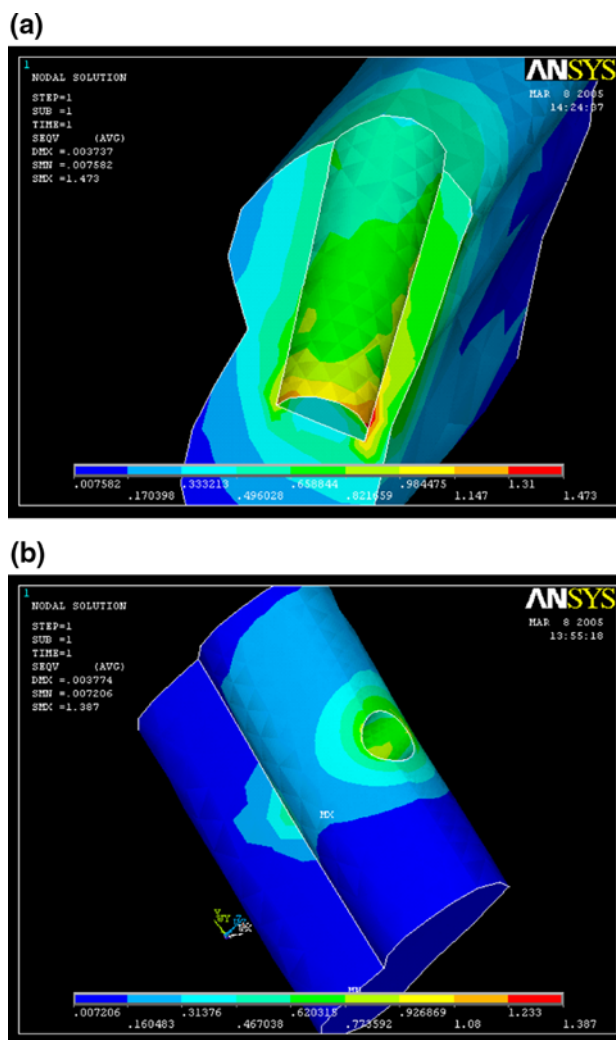


Fig. 10 a Von Mises stress in cancellous bone of Model 1, Group 1. b Von Mises stress in cancellous bone of Model 2, Group 1

Bone Implant Interface

On vertical loading, very low stress values were generated at the interface as compared to the stress values generated during non axial loading (Table 6). There were insignificant differences in the stress values generated in Model 1 and Model 2 when forces were applied in bucco-lingual and mesio-distal directions (Table 6).

Implant with Abutment

Irrespective of the loading condition and type of model, the maximum amount of stress was generated in the implant directly on the point of application of load (Fig. 13a and b Von Mises stress in implant abutment of Model 1 and Model 2, Group 1, respectively). Both the models exhibited much lesser values of stresses during axial loading when compared to stresses generated during non axial loading

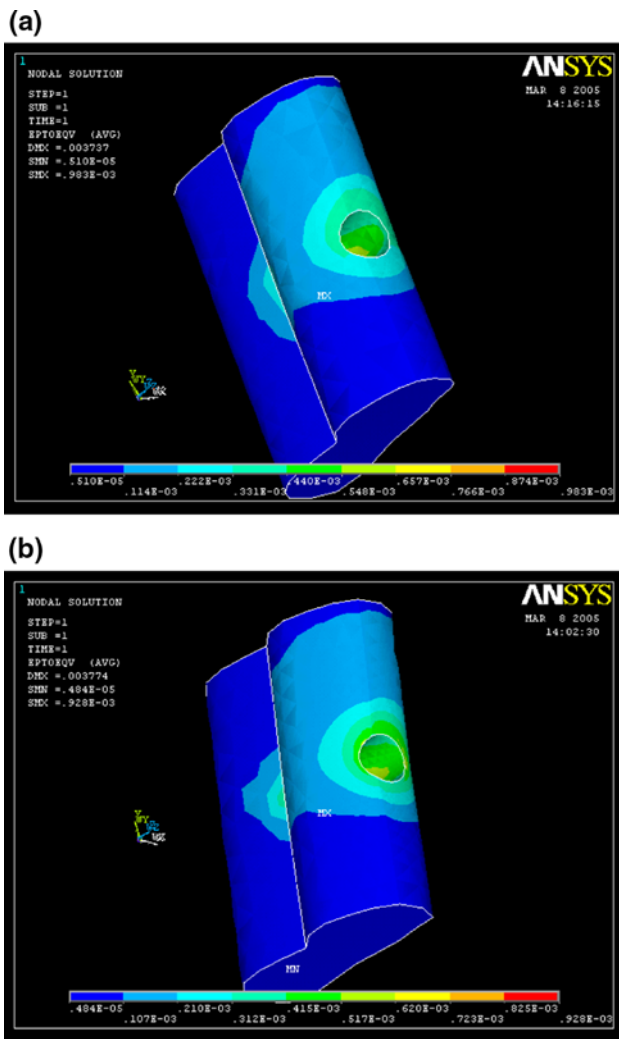


Fig. 11 a Von Mises strain in cancellous bone of Model 1, Group 1. b Von Mises strain in cancellous bone of Model 2, Group 1

(Table 7). Von Mises stresses generated in Model 2 were slightly lower than that of Model 1 when forces were applied in horizontal direction (Table 7).

Discussion

Implant failures predominantly occur because of biomechanical factors [4] so many alterations to the surface topography of the implants have been done to overcome these biomechanical factors [5, 6, 8, 31]. Although it is relatively easy to design an implant that will bear the loads that it will encounter in the course of its lifetime, it is quite another matter to design an implant that will distribute loads at a desirable level of stress to the surrounding bone. Therefore, in this study an implant design that utilizes porous surface coat layer of sintered Ti-6Al-4 V spherical

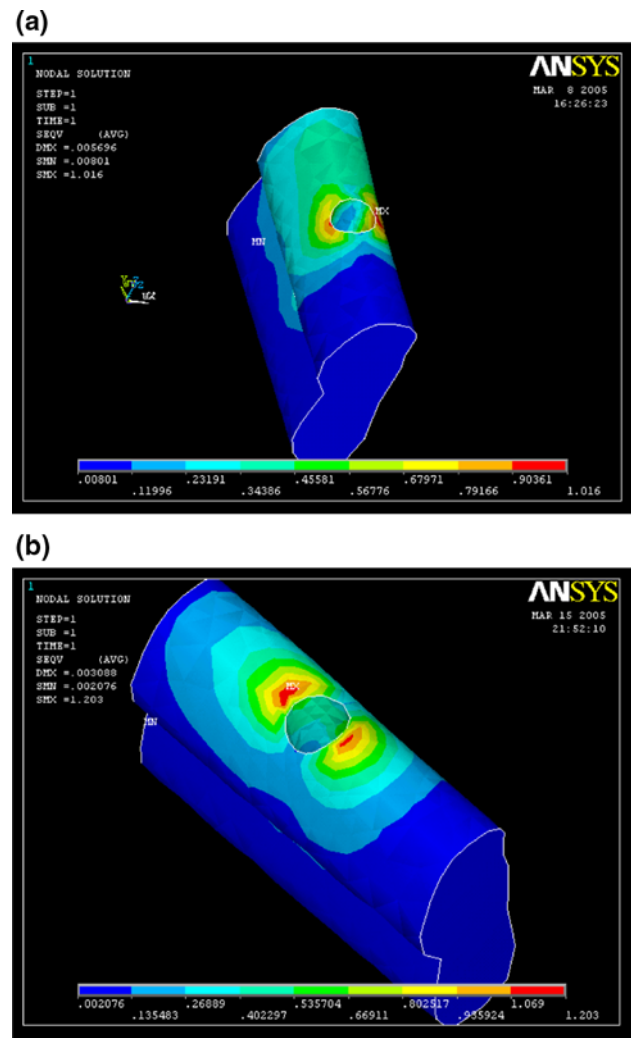


Fig. 12 a Von Mises stress in cancellous bone of Model 1, Group 2. b Von Mises stress in cancellous bone of Model 1, Group 3

powder particles has been introduced and is considered to uniformly distribute the stress along the bone implant interface [8, 10].

For ethical reasons, in vivo strain gauge measurements cannot be done inside the bone, so finite element analysis was used to measure the stress along implant bone interface [32, 33]. This method allows us to safely predict stress distribution in the contact area of the implants with cortical bone and around the apex of the implants in trabecular bone. Cook et al. [15] conducted a 3-D Finite Element analysis of a porous-rooted Co–Cr–Mo alloy dental implant to investigate the biomechanical response. 2-D Finite Element Method is not a valid representation of clinical situation. Therefore, to suit the aims of this study 3-D Finite Element Method, which can be used appropriately in asymmetric situations such as in the mandible, was used to evaluate the stresses/strains in the bone around the implant.

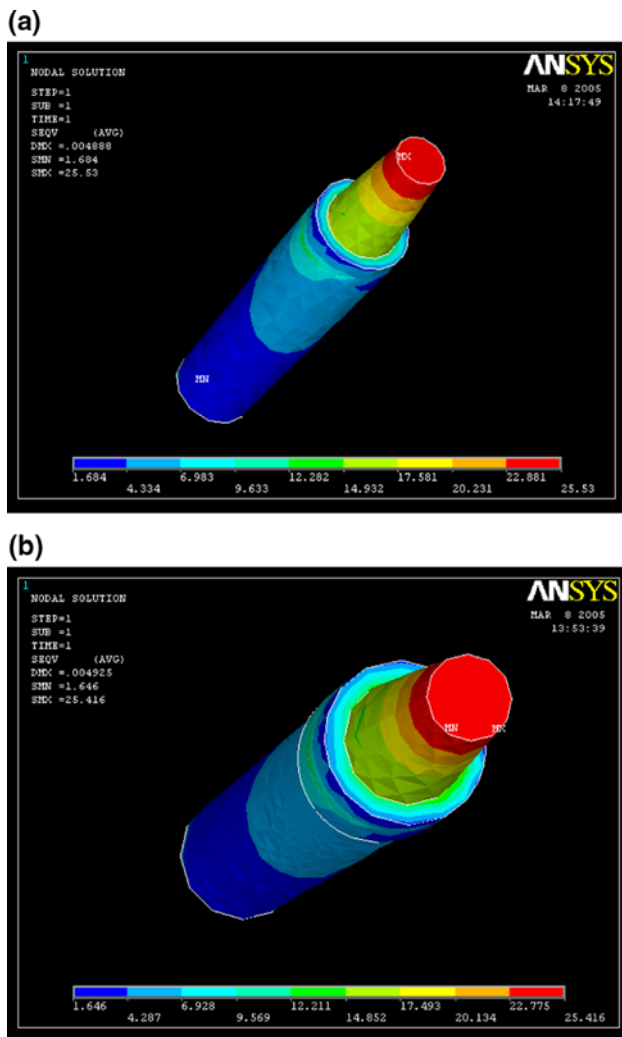


Fig. 13 a Von Mises stress in implant abutment of Model 1, Group 1. b Von Mises stress in implant abutment of Model 2, Group 1

Model Considerations

In this study, a segment of bone was modeled to simulate the posterior region of the mandible because simulation of the whole mandibular body is very elaborate. Sato et al. [7] reported in a three dimensional study, that variations in the bone stress around an implant was negligible if the length of bone between implant and segment end was at least 4.2 mm. Since in the present study this length was 12.8 mm, the end effects were considered to be negligible and did not alter the results. The size of the implant chosen best suited the dimensions of bone segment. The porous surface topography (microspheres and porosities) was generated through CAD software (Fig. 4 Model of implant with microspheres) but could not be meshed because of its complex geometry. Therefore, a model (Fig. 5 Model of implant bone ingrowth bonded interface), which accounts for the mechanics of bone grown into a porous implant

surface was generated and incorporated into the finite element analysis. This procedure simplified the meshing of the model and analysis of the results. Also to reduce the complexity of the model, prosthesis was not considered in the design of model [13].

Material Properties

The cortical bone, cancellous bone and implant with abutment were presumed to be linearly elastic, homogeneous and isotropic [6, 16]. Although cortical bone has anisotropic [17] material characteristics and possess regional stiffness variation, they were modeled isotropically due to the nonavailability of sufficient data and difficulty in establishing the principal axis of anisotropy. The mechanical properties of the interface material were mathematically calculated under the assumption that it was a composite material [18].

Loads and Constraints

The constraints at the end of the bone segment and force application on top of the abutment approximated only roughly the complex balance between masticatory forces and their reactions. These simplifications result from limitations of the modeling procedure and thus give only a general insight into the tendencies of stress/strain variations under average conditions, without attempting to simulate individual clinical situations. Although this simplification could be expected to bring about quantitative changes in the results, it was not expected to influence them qualitatively. Therefore, it is advisable to focus on qualitative comparison rather than quantitative data from these analyses [6].

Stress/Strain Distribution

Stress concentration was evident around the implant neck at the cortical bone level in all of the models. This finding was consistent with the results [16, 20, 22, 31] from other Finite Element studies as well as with findings from in vitro and in vivo experiments and clinical studies [34], which demonstrated bone loss initiating around the implant neck. The reason may be because of high modulus of elasticity of cortical bone ($E = 13,700$ MPa), which provides more rigidity and thus more capability to withstand stress.

Cortical Bone

On axial loading, stress generated in the cortical bone was comparable in both the smooth and rough surface implant (Table 3). The probable reason could be that the osseointegration assumed for both the models was 100%. According to the some clinical studies [10], it was found

that smooth surface implants have lesser osseointegrated surface as compared to an implant with rough surface. Therefore, a new 3D finite element study should be carried out where modeling of bone–implant interface should incorporate the actual osseointegrated surface of an implant to provide more realistic results.

Minimum amount of stress was generated in the cortical bone during axial loading as compared to during non axial loading. This is because the load is applied parallel to the long axis of the implant, where the ability of the implant and cortical and cancellous bone to withstand stress is more.

During bucco-lingual loading, stress seen in the cortical bone was less with Model 1 compared to Model 2. This is because of the decrease in the cross-sectional diameter of the implant to incorporate the interface. The same reason is true for increased stress component in Model 2 during mesio-distal loading.

Cancellous Bone: Stress and Strain

There was a decrease in stress magnitude during axial loading in Model 2 as the interface absorbs the stress component simulating the function of periodontal ligament in natural teeth [35]. It also distributes stress amongst the implant and the cortical bone and thus, minimizes the load on cancellous bone. It also prevents punching stress at the base of implant as seen in Model 1 (Fig. 10a Von Mises stress in cancellous bone of Model 1, Group 1), limiting the stress distribution pattern in the coronal half of the implant.

During bucco-lingual and mesio-distal loading, the stress was found to be more in Model 2, reason could be the direction of force perpendicular to the long axis of the interface. This interface has very low elastic modulus compared to implant, thus it undergoes bending with no contribution in resisting deformation leading to increased stress levels in cancellous bone.

Because of the low modulus of elasticity of cancellous bone, the load bearing capacity decreases while elasticity increases. Thus, more strain can be seen especially during horizontal loading. Von Mises strain value of cancellous bone during axial loading is similar to the value obtained during horizontal loading but with double the load i.e. 100 N. This is because of the presence of interface acting as periodontal ligament.

Bone–Implant Interface

The bone–implant interface was capable of withstanding and absorbing the stress during axial loading. This could be because the direction of force is along its long axis [35]. But during bucco-lingual and mesio-distal loading, it showed maximum stress due to high bending moments.

Thus, effectiveness of interface is visualized during axial loading [29, 36].

Implant with Abutment

Irrespective of the direction and magnitude of loading, implant with abutment withstood maximum amount of stress compared to any other component of the model. The probable reason could be its high elastic modulus ($E = 110,000$ MPa), which is 8 times the elastic modulus of cortical bone ($E = 13700$ MPa) and 80 times the elastic modulus of cancellous bone ($E = 1370$ MPa).

During axial loading, stress generated within the implant was least as compared to the stress generated during bucco-lingual and mesio-distal loading. The reason being the direction of load along the long axis of the implant provides maximum cross-sectional area to withstand the stress. The same is true for the variation in stress generated between Model 1 and Model 2, during non axial loading.

Clinical Implications

It is clear from the results of the study that the implant with porous surface tends to favor uniform stress distribution as compared to implant with smooth surface which showed high punching stress at the base of the implant [36]. Therefore, surface topography of the implant should be considered as an important factor for implant longevity.

Non-axial loading has been related to marginal bone loss, failure of osseointegration and even failure of the implant [27]. Therefore, meticulous care should be taken while planning the occlusion for implant-supported prosthesis. Occlusal contacts that distribute stress axially should be incorporated in the prosthesis. During eccentric movements the implant-supported prosthesis should allow only minimal functional contact to avoid forces from non-axial direction [37, 38].

Limitations of Finite Element Method

Even though Finite Element Method is an accurate and precise method for analyzing structures, the present study had certain limitations. The implant was assumed to be 100% osseointegrated, which is never found in clinical situation [39]. The cortical bone, cancellous bone and the implant were considered to be isotropic and lastly the static loads that were applied differed from the dynamic loading encountered during function. Therefore, further studies can be carried out with improvements made to the finite element models, applying dynamic loading conditions and

providing some movement between the parts of the model using some friction coefficient [40].

Conclusion

Despite the limitations of the methodology, it can be concluded that porous surface topography appeared to distribute stress in a more uniform pattern around the implant. The interface was considered to simulate the shock absorbing behavior of periodontal ligament of natural dentition because in the present study there was a near absence of stress in the apical region of the rough surface implant whereas the smooth surfaced implant showed high punching stress at the apex of the implant. Thus, the interface was assumed to transfer the stresses in a more uniform way around the implant. Maximum amount of stress concentration was observed in the cortical bone irrespective of the magnitude and direction of loading. Therefore cortical bone plays a major role in the dissipation of the stress. Higher stress was generated in the bone implant system during non-axial loading, which indicates the bone implant interface was somewhat less effective in stress distribution when loaded in a horizontal direction. There was favorable distribution of stress and strain pattern during axial loading.

References

- Davis DM (1998) The shift in the therapeutic paradigm: osseointegration. *J Prosthet Dent* 79:37–42
- Wyatt CCL, Zarb GA (1998) Treatment outcomes of patients with implant-supported fixed partial prostheses. *Int J Oral Maxillofac Implant* 13:204–211
- Geng JP, Tan KBC, Liu GR (2001) Application of finite element analysis in implant dentistry: a review of the literature. *J Prosthet Dent* 85:585–598
- Skalak R (1983) Biomechanical considerations in osseointegrated prosthesis. *J Prosthet Dent* 49:843–848
- Cochran DL (1999) Comparison of endosseous dental implant surfaces. *J Periodontol* 70:1523–1539
- Tada S, Stegaroiu R, Kitamura E, Miyakawa O, Kusakari H (2003) Influence of implant design and bone quality on stress/strain distribution in bone around implants: a three dimensional Finite Element Analysis. *Int J Oral Maxillofac Implant* 18:357–368
- Teixeira ER, Sato Y, Akagawa Y, Shindoi N (1998) A comparative evaluation of mandibular finite element models with different lengths and elements for implant biomechanics. *J Oral Rehabil* 25:299–303
- Levy D, Deporter DA, Pilliar RH, Watson PA, Valiquette N (1996) Initial healing in the dog of submerged versus non-submerged porous-coated endosseous dental implants. *Clin Oral Impl Res* 7:101–110
- Levy D, Deporter DA, Watson PA, Pilliar RM (1996) Periodontal parameter around porous-coated dental implants after 3 to 4 years supporting overdentures. *J Clin Periodontol* 23:517–522
- Weiss CM, Weiss A (2001) Principles and practice of implant dentistry, 1st edn. Mosby Inc, St. Louis, pp 43–44
- Wong C (2003) Oral implant innovations and methods. *Implant guide* ed 1. Japan, pp 213–215
- Brosh T, Pilo R, Sudai D (1998) The influence of abutment angulation on strains and stresses along the implant/bone interface: comparison between two experimental techniques. *J Prosthet Dent* 79:328–334
- Canay S, Hersek N, Akpinar I, Zulfu A (1996) Comparison of stress distribution around vertical and angled implants with Finite Element Analysis. *Quintessence Int* 27:591–598
- Sato Y, Teixeira ER, Tsuga K, Shindoi N (1999) The effectiveness of element downsizing on a three-dimensional finite element model of bone trabeculae in implant biomechanics. *J Oral Rehabil* 26:640–643
- Cook SD, Klawitter JJ, Weinstein AL (1982) A model for the implant-bone interface characteristics of porous dental implants. *J Dent Res* 61:1006–1009
- Stegaroiu R, Sato T, Kusakari H, Miyakawa O (1998) Influence of restoration type on stress distribution in bone around implants: a three dimensional Finite Element Analysis. *Int J Oral Maxillofac Implant* 13:82–90
- O'Mahony AM, Williams JL, Katz JO, Spencer P (2000) Anisotropic elastic properties of cancellous bone from a human edentulous mandible. *Clin Oral Implants Res* 11:415–421
- Phaneesh KR (2000) Material science and metallurgy, 1st edn. Sudha Publications, Bangalore, pp 152–162
- Rho JY, Ashman RB, Turner CH (1993) Young's modulus of trabecular and cortical bone material: ultrasonic and microtensile measurements. *J Biomech* 26(2):111–119
- Papavasiliou G, Kamposiora P, Bayne S, Felton D (1996) Three dimensional Finite Element Analysis of stress distribution around single tooth implants as a function of bony support, prosthesis type and loading during function. *J Prosthet Dent* 76:633–640
- Akca K, Iplikcioglu H (2001) Finite element stress analysis of the influence of staggered versus straight placement of dental implants. *Int J Oral Maxillofac Implants* 16:722–730
- Miejer HJA, Starmans FJM, Steen WHA, Bosman F (1993) A three dimensional Finite Element Analysis of bone around dental implants in an edentulous human mandible. *Arch Oral Bio* 6:491–496
- Meijer HJA, Starmans FJM, Bosman F, Steen WHA (1993) A comparison of three finite element models of an edentulous mandible provided with implants. *J Oral Rehabil* 20:147–157
- Hobkirk JA, Havthoulas TK (1998) The influence of mandibular deformation, implant numbers and loading position on detected forces in abutments supporting fixed implant superstructures. *J Prosthet Dent* 80:169–174
- Gibbs CH, Mahan PE, Lundeen HC, Brehnan K, Walsh EK, Holbrook WB (1981) Occlusal forces during chewing and swallowing as measured by sound transmission. *J Prosthet Dent* 46:443–449
- Zyl PPV, Grundling NL, Jooste CH (1995) Three-dimensional finite element model of a human mandible incorporating six osseointegrated implants for stress analysis of mandibular cantilever prostheses. *Int J Oral Maxillofac Implant* 10:51–57
- Barbier L, sloten JV, Krzesinski G, Schepers E, Perre GV (1998) Finite Element Analysis of non-axial versus axial loading oral implants of the mandible in the dog. *J Oral Rehabil* 25:847–858
- Cruz M, Wassall T, Taledo EM, Barra LPS, Lemonge ACC (2003) Three dimensional Finite Element Stress Analysis of Cuneiform-geometry implant. *Int J Oral Maxillofac Implants* 18:675–684
- Miejer HJA, Starmans FJM, Putter CD, Blitterswijk CAV (1995) The influence of a flexible coating on the bone stress around dental implants. *J Oral Rehabil* 22:105–111

30. Richter EJ (1995) In vivo vertical forces on implants. *Int J Oral Maxillofac Implants* 10:99–107
31. Rieger HR, Adams WK, Kinzel GL (1990) A Finite Element survey of eleven endosseous implants. *J Prosthet Dent* 63: 457–465
32. Akca K, Cehreli MC, Iplikcioglu H (2002) A comparison of three dimensional FEA with in vitro strain gauge measurements on dental implants. *Int J Prosthodont* 15:115–121
33. Benzing UR, Gall IH, Weber IH (1995) Biomechanical aspects of two different implant prosthetic concepts for edentulous maxillae. *Int J Oral Maxillofac Implants* 10:188–198
34. Vollmer D, Meyer U, Joos U, Vegh A, Piffko J (2000) Experimental and finite element study of a human mandible. *J Cranio-maxillofac Surg* 28(2):91–96
35. Rees JS (2001) An investigation into the importance of the periodontal ligament and alveolar bone as supporting structures in Finite Element studies. *J Oral Rehabil* 28:425–432
36. Weinstein AL, Klawitter JJ, Subhash CA, Schuessler R (1976) Stress analysis of porous rooted dental implants. *J Dent Res* 55:772–777
37. Cehreli MC, Iplikcioglu H (2002) In vitro strain gauge analysis of axial and off-axial loading on implant supported fixed partial dentures. *Implant dentistry* 11:286–292
38. Kaukinen JA, Edge MJ, Lang BR (1996) The influence of occlusal design on simulated masticatory forces transferred to implant retained prosthesis and supporting bone. *J Prosthet Dent* 76:50–55
39. Wadamoto M, Akagawa Y, Sato Y, Kubo T (1996) The 3D bone interface of an osseointegrated implant. I: a morphometric evaluation in initial healing. *J Prosthet Dent* 76:170–175
40. Lang LA, Byungsik K, Wang RF, Lang BR (2003) Finite Element Analysis to determine implant preload. *J Prosthet Dent* 90:539–546